American Mineralogist, Volume 92, pages 587–597, 2007

Characterization of defects and the local structure in natural and synthetic alunite (K, Na, $H_3O)Al_3(SO_4)_2(OH)_6$ by multi-nuclear solid-state NMR spectroscopy

Ulla Gro Nielsen,[1] Juraj Majzlan,[2] Brian Phillips,[3] Martine Ziliox,[4] and Clare P. Grey[1,*]

[1]Department of Chemistry and Center for Environmental Molecular Science, SUNY Stony Brook, Stony Brook, New York 11794-3400, U.S.A.
[2]Institute for Mineralogy and Geochemistry, Albert-Ludwigs University of Freiburg, Albertstrasse 23b, Freiburg, D-79104, Germany
[3]Department of Geosciences and Center for Environmental Molecular Science, SUNY Stony Brook, Stony Brook, New York 11794-2100, U.S.A.
[4]Center for Structural Biology, SUNY Stony Brook, New York 11794-5115, U.S.A.

Abstract

The local structural environments in a series of natural and synthetic alunite samples [ideally $AAl_3(SO_4)_2(OH)_6$, $A = H_3O^+$, D_3O^+, Na^+, and K^+] have been probed by solid-state ^1H, ^2H, ^{23}Na, ^{27}Al, and ^{39}K NMR spectroscopy. The natural alunite [$KAl_3(SO_4)_2(OH)_6$] and synthetic hydronium alunite samples contain few structural defects, whereas the synthetic natroalunite and alunite samples have ca. 10% Al vacancies based on ^{27}Al NMR. A new ^{27}Al local environment (Al_D) was observed and assigned to Al with one Al vacancy in the first cation sphere. Three different proton environments, Al_2-OH, Al-OH_2, and H_3O^+ are detected by ^1H and ^2H MAS NMR. The hydronium ion (H_3O^+) is only observed in hydronium alunite, and is associated with the stoichiometric regions of the sample. It was not detected in ^1H and ^2H NMR spectra of alunite and natroalunite despite K (Na) occupancies of significantly less than 100%, as determined from elemental analysis. Thus, our NMR results suggest that the common assumption, namely that an *A* vacancy and an Al^{3+} vacancy are compensated by adding an H_3O^+ and 3 H^+ (creating 3 Al-OH_2 groups), respectively, is too simplistic. Instead, a significant fraction of the Al^{3+} vacancies are compensated for by 4 H^+ ions, resulting in 4 Al-OH_2 groups per vacancy. This substitution is accompanied by the simultaneous deprotonation of a H_3O^+ ion present on the *A* site. The resultant H_2O molecule is unnecessary for charge balance, accounting for the *A*-site deficiency often observed. The presence of Al^{3+} and A^+ vacancies appears closely correlated based on NMR.

Keywords: Alunite, solid-state NMR, hydronium ion, ^{23}Na NMR, ^{27}Al NMR, ^1H NMR, ^2H NMR, ^{39}K NMR

Introduction

The alunite [$AAl_3(SO_4)_2(OH)_6$, $A = H_3O^+$, Na^+, and K^+] and jarosite [$AFe_3(SO_4)_2(OH)_6$] series are members of the large alunite group of minerals and related compounds that are relevant in several areas of science, including environmental chemistry (Stoffregen et al. 2000) and materials science (Greedan 2001). These minerals are commonly precipitated from acidic mine waters or acidic hydrothermal solutions (Stoffregen et al. 2000). They are also used in hydrometallurgy, especially in processing of Zn and U ores (Dutrizac and Jambor 2000). Monovalent and divalent metal ions including Pb^{2+}, Cd^{2+}, and Tl^+ may be co-precipitated and incorporated in the structure of these minerals, resulting in removal and immobilization of these species from the aqueous environment. Moreover, the magnetic ions in the jarosite structure are located in nodes of a Kagomé lattice and the magnetic properties of these compounds have received much attention (Greedan 2001; Harrison 2004; Nocera et al. 2004). In addition, the identification of jarosite on Mars has been taken as evidence for aqueous processes on the planet (Klingelhöfer et al. 2004; Madden et al. 2004; Squyres et al. 2004).

Minerals of the alunite group crystallize in space group $R\bar{3}m$. Their general formula is $AB_3(SO_4)_2(OH)_6$, where $B = Fe^{3+}$, Al^{3+}, V^{3+}, Cr^{3+}... and $A = H_3O^+$, Na^+, K^+, Rb^+, Cs^+, Ag^+, ½ Pb^{2+}, NH_4^+... (Dutrizac and Jambor 2000). Synthetic and natural members of this group generally exhibit considerable non-stoichiometry and contain structural defects on the *B* site. The presence of these defects may significantly affect the magnetic properties of phases where $B = Fe^{3+}$, V^{3+} and Cr^{3+} as well as the ion exchange capabilities of jarosite (Kurata et al. 1984; Ozeki et al. 1989). Substantial numbers of vacancies are also found at the A^+ site, which usually has an occupancy of 80–95% (Greedan 2001). A further complication is the presence of excess water molecules (~1 H_2O per unit formula) (Ripmeester et al. 1986; Bohmhammel et al. 1986; Drouet and Navrotsky 2003; Drouet et al. 2004). Recently, synthesis procedures for stoichiometric transition metal jarosite have been reported (Grohol and Nocera 2002; Grohol et al. 2003).

The structure of alunite (Fig. 1) consists of sheets of $AlO_2(OH)_4$ octahedra. The sheets are decorated by sulfate tetrahedra, and the A^+-ions are located between the sheets. The six ligands coordinated to Al^{3+} include four equatorial OH groups shared between the neighboring Al^{3+} ions (denoted as Al_2-OH in this paper) and two axial O atoms of sulfate groups above and

* E-mail: cgrey@notes.cc.sunysb.edu

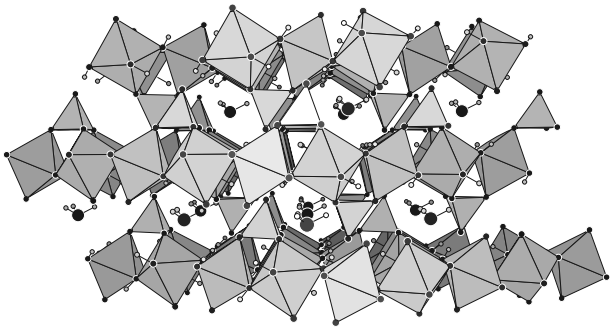

FIGURE 1. Polyhedral representation of the crystal structure of hydronium alunite $[(H_3O)Al_3(SO_4)_2(OH)_6]$ viewed along the a axis and illustrating the porous structure of this compound. The proton locations are from the isostructural hydronium jarosite.

below the octahedral sheet. The monovalent ions are coordinated by 12 O atoms or hydroxyl groups. There are weak hydrogen bonds between the Al_2-OH groups and the O atoms in the sulfate tetrahedron that point towards the cavity (Wang et al. 1965; Schukow et al. 1999; Lager et al. 2001).

A stoichiometric alunite structure contains a single Al^{3+} crystallographic site denoted here as Al1. The structure also contains a single *A* (*A* = Na^+, K^+, H_3O^+) site (Wang et al. 1965; Schukow et al. 1999; Lager et al. 2001). Thus, the ^{27}Al, ^{23}Na, and ^{39}K NMR spectra of a stoichiometric alunite will each consist of a single NMR resonance. A ^1H NMR spectrum of a stoichiometric alunite with *A* = Na^+, K^+ will contain resonances from the Al_2-OH groups only, whereas that of a pure hydronium alunite will contain Al_2-OH and H_3O^+ resonances in a ratio of 2:1. Deviation from the ideal stoichiometry and the presence of structural defects results in the formation of additional Al, *A*, and H environments, as discussed below. An introduction of Al vacancies (i.e., at the *B* site) can create several local environments, one of which is shown in Figure 2. A vacancy at the *B* site is thought to be compensated by 3 H^+ to maintain charge balance:

$$Al(OH)_4O_2 + 3H^+ = \square(OH_2)_3(OH)O_2 + Al^{3+} \quad (1)$$

forming water molecules coordinated to the Al atoms (Al_D) adjacent to the vacancy, i.e., Al_D-OH_2 groups. However, an Al vacancy creates four terminal Al-OH groups, as illustrated in Figure 2, and it is possible that all four groups become protonated, the fourth proton being compensated by a vacancy or hydronium ion on the *A* site:

$$Al(OH)_4O_2 + 3H^+ + H_3O^+ \rightarrow \square^+(OH_2)_4O_2 + H_2O + Al^{3+} \quad (2)$$

An alternative to this simple, static model for charge compensation is a dynamic model that includes chemical exchange. For example, the protons could hop between four (or more) sites in the structure. Such a model will be difficult to investigate with diffraction techniques. Solid-state NMR spectroscopy is a versatile probe of local structure, but also of molecular dynamics and chemical exchange processes spanning a large range of time scales from µs to min. For example, ^2H MAS NMR can be used to probe to motion from the time scale of the ^2H quadrupole interaction (µs to s) (Maricq and Waugh 1979; Spiess 1983; Weintraub and Vega 1995).

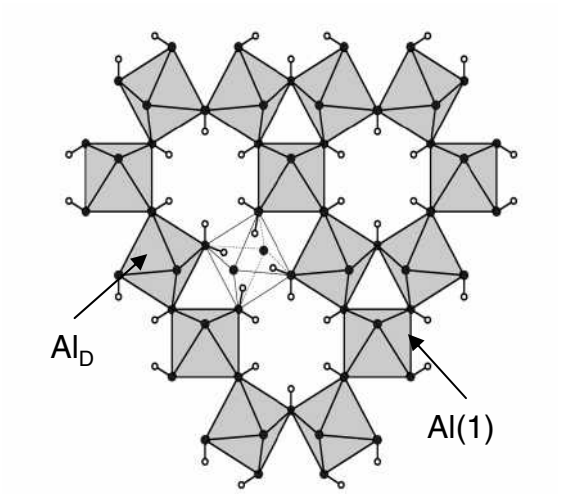

FIGURE 2. The local structure in the octahedral layers near an Al vacancy. A new Al site, Al_D, is the next nearest neighbor to a vacancy site.

It is still a matter of debate as to whether the hydronium ion exists in the alunite structure or whether it reacts with a basic site and is converted to H_2O. Only the oxygen position of the H_3O^+ ion has been reliably determined by diffraction studies (Lager et al. 2001; Majzlan et al. 2004), as the hydrogen positions appear disordered. Chemical analysis can determine the Na^+ and K^+ contents, but not the method of charge compensation (e.g., presence of H_3O^+ or substitution of OH_2 for OH^- ligands). Because the calculated occupancy of the *A* site by Na^+ and K^+ is rarely equal to 1.0, an H_3O^+ ion is assumed to be present at the A^+ site. This allows the fraction of H_3O^+ on the A^+ site to be calculated as $1 - (Na^+ + K^+)$. However, even the A^+ site may not be fully occupied, as recently demonstrated for hydronium jarosite where an occupancy of 91% was determined by single-crystal X-ray diffraction (Majzlan et al. 2004). This uncertainty in *A*-site occupancy complicates the question of the H_3O^+ existence and the determination of the correct chemical composition of alunite.

Vibrational studies yielded ambiguous results, because the vibrational bands of H_2O and H_3O^+ overlap (Lager et al. 2001; Bishop and Murad 2005). Solid-state ^1H and ^2H NMR spectroscopy has proven the most successful technique for probing the local proton environments and for identifying the hydronium ion in alunite due to the distinctive chemical shift (Bohmhammel et al. 1986; Ripmeester et al. 1986). Several different proton/deuteron environments including H_3O^+, Al_2-OH, and Al-OH_2 have been observed by Ripmeester et al. (1986) and Bohmhammel et al. (1986). Kydon et al. (1968) suggested the existence of the hydronium ion in the hydronium gallium jarosite compound based on variable temperature measurements of proton relaxation rates (T_1) and analysis of the second moments of ^1H NMR spectra.

To our knowledge, no solid-state ^{27}Al NMR data have been reported for alunite despite the widespread application of solid-state ^{27}Al NMR in studies of synthetic materials and minerals. The sensitivity of ^{27}Al NMR to local structural environment should make it a useful probe for the average and defect structures in the alunite series, complementing previous work using

^{1}H and ^{2}H NMR in these materials (Bohmhammel et al. 1986; Ripmeester et al. 1986). Here we report the results from multi-nuclear ^{1}H, ^{2}H, ^{23}Na, ^{27}Al, and ^{39}K NMR spectroscopic study of a series of synthetic and natural alunite samples, both near- and non-stoichiometric. Structural defects are readily observed in these solid-state NMR spectra. Moreover, the presence of H_3O^+ is closely linked to the number of structural defects and readily probed by high-speed ^{1}H MAS NMR spectroscopy.

Experimental methods

Synthesis

All synthetic samples were prepared from mixtures of H_2O (deionized), D_2O (99.8% isotopic, Alfa-Aesar), K_2SO_4 or Na_2SO_4 (reagent grade, Fisher), and $Al_2(SO_4)_3(H_2O)_x$ ($x \approx 17$, reagent grade, Alfa Aesar). The initial composition of all mixtures is given in Table 1. For the synthesis of the deuterated samples, $Al_2(SO_4)_3(H_2O)_{\sim 17}$ was partially dehydrated by heating at 110 °C for 20 minutes; followed by 250 °C for 1 hour and 450 °C for 1 hour in a Pt crucible. In every case, all solids completely dissolved in water. The solution was then sealed in a stainless steel Parr vessel with a teflon liner (45 or 125 mL internal volume). The vessel was placed in an oven at the temperature and time specified in Table 1. Afterwards, the vessel was allowed to cool under a stream of air, and the sample was separated from the solution by filtration, dried at 40 °C and gently ground. Partially deuterated samples were prepared by mixing D_2O with fully hydrated or partially dehydrated starting chemicals. Samples are labeled according to the convention *A*-Alu, where *A* = H_3O, D_3O, Na or K. *A*-Alu-D refers to the deuterated alunite and natroalunite samples.

A highly crystalline, natural alunite specimen (Nat-Alu) was also examined. A few single crystals (ca. 2 × 2 × 4 mm) were selected from a specimen from the Chinkuahshih mine in Taiwan, then crushed and ground to a fine powder before NMR experiments. This sample was chosen because the crystals were easy to separate from the matrix, therefore providing a pure specimen. However, such well-crystalline samples are not common and the sample may not represent most of the natural occurrences. However, we have attempted to study "more typical" alunite samples. These were found to be contaminated with other minerals to such an extent that the interpretation of NMR spectra was ambiguous.

X-ray diffraction

Powder X-ray diffraction (XRD) patterns were collected with a Bruker AXS D8 Advance diffractometer, employing Cu*K*α radiation and a graphite monochromator. Phase purity of the samples was checked and the lattice parameters calculated by profile fits using GSAS (Table 1) (Larson and von Dreele 1994).

Elemental analysis

The samples (~50 mg) were dissolved in 20 mL of distilled 4 N HCl in a microwave digestor. After the digestion, the samples were analyzed for Na, K, and Al by atomic absorption spectroscopy (Analytik Jena, AAS Vario 6 spectrometer), and for SO_4^{2-} by ion chromatography (Dionex DX 120). The results from elemental analysis are shown in Table 1.

NMR spectroscopy

Solid-state ^{1}H, ^{23}Na, and ^{27}Al NMR experiments were performed on a Bruker Avance 600 NMR spectrometer using 2.5 mm H/FX and 4 mm HFX MAS NMR probes with spinning speeds in the range 25–35 and 10–14 kHz, respectively. Solid-state ^{2}H and ^{39}K MAS NMR spectra were recorded on a Chemagnetics Infinity Plus 500 MHz NMR spectrometer using 4 and 5 mm HX T3 MAS probes, respectively. Spectra were referenced using H_2O [$\delta_{iso}(^{1}H) = 4.8$ ppm], D_2O [$\delta_{iso}(^{2}H) = 4.8$ ppm], 1 *M* NaCl [$\delta_{iso}(^{23}Na) = 0$ ppm], 1 *M* $AlCl_3$ [$\delta_{iso}(^{27}Al) = 0$ ppm], and $KBr_{(s)}$ [$\delta_{iso}(^{39}K) = 55$ ppm] as with external standards. r.f.-field calibrations were performed using these standards or the sample. The magic-angle was carefully set by minimizing the line width of spinning side bands (ssbs) from the satellite transitions for the ^{23}Na resonance from $NaNO_3$, ^{2}H from CD_3COONa, or from ^{79}Br in KBr depending on the actual configuration of the probe. ^{1}H and ^{39}K MAS NMR spectra were recorded using a Hahn-echo sequence to suppress ^{1}H background signals and probe ringing, respectively. Additional ^{1}H MAS NMR spectra were recorded at 9.4 T (400 MHz) using a 4 mm H/FX MAS probe with a limited ^{1}H background using 10–14 kHz spinning speeds. ^{2}H, ^{23}Na, and ^{27}Al NMR spectra were recorded using short (0.3–1 µs, 10–20°) pulses to ensure uniform and quantitative excitation. ^{27}Al 3QMAS NMR (Frydman and Harwood 1995) spectra were obtained using the 3 pulse z-filter sequence (Massiot et al. 1996) with and without ^{1}H decoupling TPPM; (Bennett et al. 1995) at $\gamma B_1/2\pi$ (^{1}H) ≈ 90 kHz. Several ^{27}Al hetero-nuclear correlation (HETCOR) NMR spectra were recorded with contact times in the range 40 to 150 µs, where the cross-polarization (CP) conditions were optimized on the samples.

Analyses of the NMR spectra were performed with DMFit (Massiot et al. 2002), STARS (^{2}H) (Skibsted et al. 1991), and WinSolids (^{39}K NMR) developed by Klaus Eichele. Simulations of quadrupole tensor distributions were performed by using the method of Coster et al. (1994).

Results and discussion

^{27}Al MAS and 3QMAS NMR

Synthetic hydronium and deuteronium alunite (H_3O-Alu and D_3O-Alu). The experimental ^{27}Al MAS NMR spectrum of

Table 1. Chemical composition of the solutions, from which the alunite samples were precipitated, and composition of the solid samples determined from elemental analysis

Sample	Starting composition of the synthesis solution	Synthesis conditions	Sample composition* (normalized to $2SO_4$)		Lattice parameters (Å)
K-Alu	37 mL H_2O, 1.50 g K_2SO_4, 6.3 g Al sulfate	70 °C, 1 hour 150 °C, 23 hours	K^+ Al^{3+} $(SO_4)^{2-}$	0.79 2.49 2	a = 7.0122(3) c = 17.146(3)
Na-Alu	37 mL H_2O, 1.84 g Na_2SO_4, 6.0 g Al sulfate	70 °C, 9 hours 140 °C, 22 hours	Na^+ Al^{3+} $(SO_4)^{2-}$	0.83 2.28 2	a = 6.9983(2) c = 16.664(1)
H_3O-Alu	25 mL H_2O, 4.5 g Al sulfate pH adjusted to 3.5 by adding $MgCO_3$ powder	ultrasonicated for 15 min; allowed to stand with stirring for 1 hour 190 °C, 2 days	Al^{3+} $(SO_4)^{2-}$	2.83 2	a = 7.0119(2) c = 17.133(1)
D_3O-Alu	1.8 g of dehydrated Al sulfate; 10 mL D_2O	sealed in a Parr vessel with a stirbar; stirred at RT overnight; 190 °C, 3 days	Al^{3+} $(SO_4)^{2-}$	3.01 2	a = 7.0111(2) c = 17.123(1)
Nat-Alu	–	natural alunite (Chinkuahshih mine, Taiwan)			a = 6.9789(9) c = 17.248(3)
Na-Alu-D	10 mL D_2O, 497 mg Na_2SO_4, 1.627 g Al sulfate	70 °C, 1 hour 130 °C, 23 hours			a = 6.9964(4) c = 16.667(1)
K-Alu-D	14.5 mL D_2O, 15.5 mL H_2O 1.22 g K_2SO_4, 5.10 g Al sulfate	70 °C, 1 hour 130 °C, 23 hours			a = 7.0180(5) c = 17.125(2)

* The error of the elemental analyses is ±5%.

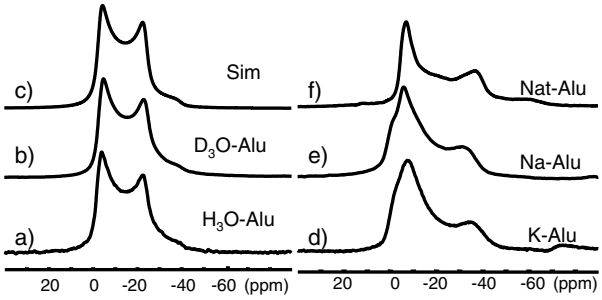

FIGURE 3. ^{27}Al MAS NMR spectra of (**a**) H_3O-Alu, (**b**) D_3O-Alu, and (**c**) simulation using the parameters in Table 2. (**d**) K-Alu, (**e**) Na-Alu, and (**f**) Nat-Alu. All experimental spectra were recorded at 14.1 T (156.37 MHz) using 14 kHz spinning speed.

TABLE 2. ^{27}Al NMR quadrupole coupling parameters and isotropic chemical shifts for series of synthetic and natural alunites determined from analysis of MAS and 3QMAS spectra recorded at 14.1 T

Sample	δ_{iso}(ppm)	C_Q (MHz)	η_Q	Fraction
H_3O-Alu	3.4 ± 0.4	8.45 ± 0.10	0.10 ± 0.10	
D_3O-Alu	3.2 ± 0.5	8.48 ± 0.10	0.10 ± 0.10	
K-Alu, Al1	4.3 ± 1.5	10.3 ± 0.3	0.05 ± 0.10	≈ 60%
Al_D	3.2 ± 1.5	6.0 ± 0.3	0.75 ± 0.10	≈ 34%
Al_{I1}	2.2 ± 0.8	4.0 ± 0.3*		≈ 3%
Al_{I2}	0.5 ± 0.5	3.3 ± 0.4*		≈ 3%
Na-Alu, Al1	5.2 ± 0.8	10.3 ± 0.50	0.08 ± 0.10	≈ 65%
Al_D	1.4 ± 1.5	6.3 ± 0.4	0.75 ± 0.10	≈ 35%
Al_{I1}	1.8 ± 0.8	2.9 ± 0.4*		<2%
Al_{I2}				<2%
Nat-Alu Al1	3.9 ± 2	10.6 ± 0.5	0.05 ± 0.10	>95%
Al_I	1.1 ± 0.7			<5%
Na-Alu-D (2.5 mm) Al1	5.0 ± 1.0	10.2 ± 0.5	0.00 ± 0.10	≈ 57%
Al_D	−1 ± 2	6.0 ± 0.5	0.65 ± 0.10	≈ 38%
Al_{I1}	−2 ± 2	3.7 ± 0.7*		≈ 5%
Al_{I2}				
K-Alu-D Al1	3.0 ± 1	10.2	0.00 ± 0.10	≈ 57%
Al_D	−1 ± 2	6.00	0.65 ± 0.15	≈ 38%
Al_{I1}	2.3 ± 0.8	4.2 ± 0.3*		<5
Al_{I2}	0.9 ± 1.0	3.7 ± 0.7*		<5%

Notes: 3QMAS NMR spectra were recorded with and without high-power ^{1}H decoupling.
* Second-order quadrupole parameter (SOQE, $SOQE = C_Q\sqrt{(1+\frac{1}{3}\eta_Q}$), determined from 3QMAS NMR spectra.

H_3O-Alu (Fig. 3a) contains a single resonance with a pronounced second-order quadrupolar line shape characteristic for a ^{27}Al site with close to axial symmetry ($\eta_Q \approx 0$). This resonance is assigned to Al1, the only Al site in a defect-free alunite (Fig. 2). A very similar spectrum is obtained for the D_3O-Alu sample, as illustrated in Figures 3a and 3b. Optimizations of the quadrupolar line shape using a model with a single site gave C_Q = 8.45(10) MHz and η_Q = 0.10(10) for H_3O-Alu (Table 2) and nearly identical parameters within the error-limits for D_3O-Alu. A significant improvement of the fit can be obtained by including a small distribution of the ^{27}Al quadrupole coupling (ca. 0.5 MHz), but the average values do not differ substantially from those given in Table 2. This small distribution in C_Q likely arises from structural distortions due to the presence of defects. Chemical shift anisotropies were not considered as spectra recorded with high spinning speeds (35 kHz) at low field (8.4 T), where chemical shift anisotropies are negligible for ^{27}Al, could also be reproduced with a distribution in C_Q. No other resonances could, however, be distinguished in ^{27}Al MAS and 3QMAS spectra recorded at 8.4, 11.7, 14.1, and 16.5 T (not shown), suggesting that the defect concentration in these samples is low.

Synthetic alunite (K-Alu) and natroalunite (Na-Alu). The ^{27}Al MAS NMR spectra of K-Alu and Na-Alu are more complex than those of H_3O/D_3O-Alu, as illustrated in Figures 3d and 3e, respectively. The higher frequency singularity is about four times higher than the lower frequency singularity, suggesting that one or more additional resonances are present. An increase in the size of the quadrupole coupling constants for Al1 is also observed, as seen by the shift of the lower frequency singularity to more negative frequencies, as compared to the same discontinuity for Al1 in H_3O-Alu.

Four different ^{27}Al resonances, denoted Al1, Al_D, Al_{I1}, and Al_{I2}, can be resolved in the 3QMAS NMR spectrum of K-Alu (Fig. 4), all in the spectral region for octahedrally coordinated aluminum (Müller et al. 1981; Smith 1993; Jansen et al. 1998). The spectrum is not necessarily quantitative due to the large variation in C_Q for the different sites and therefore in the MQ excitation and conversion efficiencies (Amoureux et al. 1996). The strong ^{1}H-^{27}Al dipolar coupling, which is scaled by the MQ order (factor of 3) in the F1 dimension, was suppressed in these experiments by high-power proton decoupling during evolution and acquisition. ^{1}H decoupling improved resolution in F1, although it resulted in a distortion of the quadrupolar line shapes especially for the Al1 resonance, as seen in Figure 4b. Spectra recorded without ^{1}H decoupling contained less distorted line shapes, but had a lower spectral resolution resulting in overlap of the Al_{I1} and Al_{I2} resonances. The NMR parameters were extracted based on the best fits to the positions of the discontinuities in the spectra (Table 2). The quadrupole coupling constant of the main resonance [Al1, C_Q = 10.6(5) MHz] is 25% larger than observed for H_3O-Alu. The asymmetry parameter and isotropic chemical shift are similar to those for the Al1 site in H_3O-Alu. The second most intense resonance detected is assigned to the defect site Al_D (see Fig. 2), which also has a substantial, but smaller quadrupole coupling, C_Q = 6.0(3) MHz, and η_Q = 0.75(10). Two additional resonances, Al_{I1} and Al_{I2}, are present, which have smaller quadrupole coupling constants and similar isotropic chemical shifts, δ_{iso} (≈ 2.2 and 0.5 ppm), second-order quadrupole products, $SOQE = C_Q\sqrt{1+\eta_Q^2/3}$), of 4.0(3) and 3.3(4) MHz as calculated from the 3QMAS spectrum. These resonances were tentatively assigned to impurities and discussed in greater detail later.

The 3QMAS NMR of Na-Alu (data not shown) is similar to that for K-Alu except that only one broad resonance (Al_I) can be identified in the region for Al_{I1} and Al_{I2} (Table 2), in addition to the more intense Al1 and Al_D resonances. These spectra are consistent with a higher concentration of aluminum vacancies and defects in both Na and K-Alu, as compared with H_3O-Alu and H_3O-Alu. The larger concentration of Al^{3+} vacancies in Na-Alu and K-Alu are in agreement with the analyzed Al:sulfate ratio in these samples (Table 1).

Natural alunite (Nat-Alu)

The natural alunite sample gives rise to a ^{27}Al MAS spectrum (Fig. 3f) with main features that are similar to those of the synthetic alunite samples, with the Al1 site predominating.

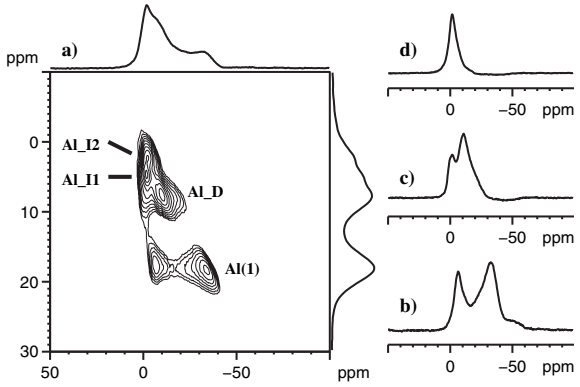

FIGURE 4. ^{27}Al 3QMAS NMR spectrum of K-Alu acquired using 90 kHz ^{1}H decoupling showing the presence of 4 different aluminum resonances. The right hand side shows sums of the region for the Al1, Al_D, and Al_{I1} sites. Proton decoupling results in distorted quadrupolar line shape for the Al1 sites with C_Q = 10.5 MHz. The convention of Amoureux and Fernandez (1998, 2000) is used for referencing the F1 dimension.

Simulations of the line shape from a slice of the 3QMAS spectrum results in δ_{iso} = 3.9(2.0) ppm, C_Q = 10.6(5) MHz, and η_Q = 0.05(10). The most noticeable difference between the natural and synthetic alunite is that the Al_D site ($C_Q \approx 6.5$ MHz) is not observed in the ^{27}Al MAS spectrum and only a weak resonance (Al_I) is observed in the 3QMAS NMR spectrum, at a position expected for the Al_{I1} or Al_{I2} sites (not shown). The data indicate that the natural sample contains very few *B*-site vacancies.

^{1}H and ^{2}H MAS NMR spectra

Hydronium alunite (H_3O-Alu). Two ^{1}H resonances with δ_{iso} = 4.0 and 10.6 ppm are readily apparent in the ^{1}H MAS NMR spectrum of hydronium alunite (Fig. 5a). They are assigned to Al_2-OH and H_3O^+ groups, in agreement with previous results (Bohmhammel et al. 1986; Ripmeester et al. 1986). Strongly hydrogen bonded groups also resonate in the high frequency region (Berglund and Vaughan 1980), but ^{2}H MAS NMR (Ripmeester et al. 1986, vide infra) indicate that the 10.6 ppm resonance is associated with a highly mobile species, excluding this possibility. A fit to the ^{1}H MAS NMR spectrum requires the inclusion of two additional weaker resonances at δ_{iso} = 6.4 and 9.5 ppm. The resonance at 6.4 ppm has been assigned to Al-OH_2 groups in previous studies (Bohmhammel et al. 1986; Ripmeester et al. 1986). Non-bound H_2O molecules usually resonate between 4 and 8 ppm, which overlaps with the chemical shift range for Al-OH_2 groups (6–10 ppm) (Berglund and Vaughan 1980; Ratcliffe et al. 1985; Akitt and Elders 1988) complicating the assignment. The 6.4 ppm resonance is broader (FWHM = 3.0 kHz) than that for the Al_2-OH group (FWHM = 1.3 kHz), which may be due to a combination of effects including ^{1}H-^{1}H homonuclear dipolar coupling, chemical exchange, molecular motion, or the presence of multiple sites. Previous ^{2}H NMR studies have shown that the individual Al-OD_2 and D_3O^+ groups remained mobile down to ca. 77 K (Ripmeester et al. 1986). To test whether any chemical exchange occurs between the Al-OH_2, H_2O, and H_3O^+ groups, variable temperature ^{1}H MAS NMR spectra were recorded from –150 to 250 °C. No significant changes were seen in this temperature range, i.e., no onset or freezing out of fast chemical exchange among Al-OH_2, H_2O, and H_3O^+ occurs.

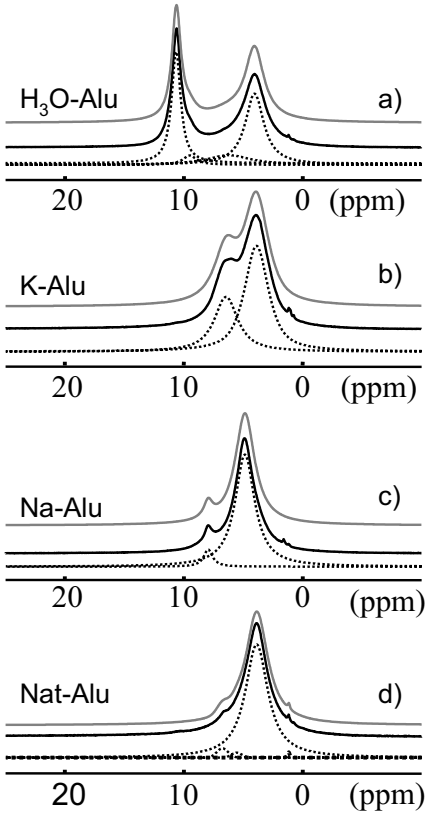

FIGURE 5. ^{1}H MAS NMR spectra of (**a**) H_3O-Alu, (**b**) K-Alu, (**c**) Na-Alu, and (**d**) Nat-Alu. In each are shown the experimental spectrum (solid black line), a simulation (solid gray line), and the individual peaks (dotted black lines) used in the fit. The parameters used in the simulations can be found in Table 1. Only the isotropic region is shown for enhanced resolution, but all spinning side bands were employed for quantification of the spectral intensity.

It is clear that ^{1}H NMR is more sensitive to the presence of small concentrations of defects than the ^{27}Al NMR spectroscopy. Using the intensities for the 10.6 and 4.0 ppm resonances, obtained from the fit of the ^{1}H MAS NMR spectrum in Figure 5a, a ratio for I(Al_2-OH):I(H_3O^+) of 1.37:1 is obtained. This value deviates significantly from the theoretical value of 2:1 based on the ideal, stoichiometric crystal structure. Structural defects and vacancies will alter this ratio significantly.

Deuterated hydronium alunite (D_3O-Alu). The experimental ^{2}H MAS NMR spectrum of deuterated hydronium alunite (Fig. 6a) shows two spinning sideband (ssb) manifolds associated with resonances at $\delta_{iso}(^{2}H)$ = 4.0(5) and 10.1(5) ppm. A quadrupole coupling constant (C_Q) of 235(9) kHz and an axial symmetric quadrupole tensor [η_Q = 0.02(5)] are obtained for the 4.0 ppm site from a least-square fit to the integrated ssb intensities. This value is in excellent agreement with values of C_Q = 240 kHz and η_Q = 0.0 obtained from ^{2}H static NMR by Ripmeester et al. (1986). Using the correlation between ^{2}H quadrupole coupling

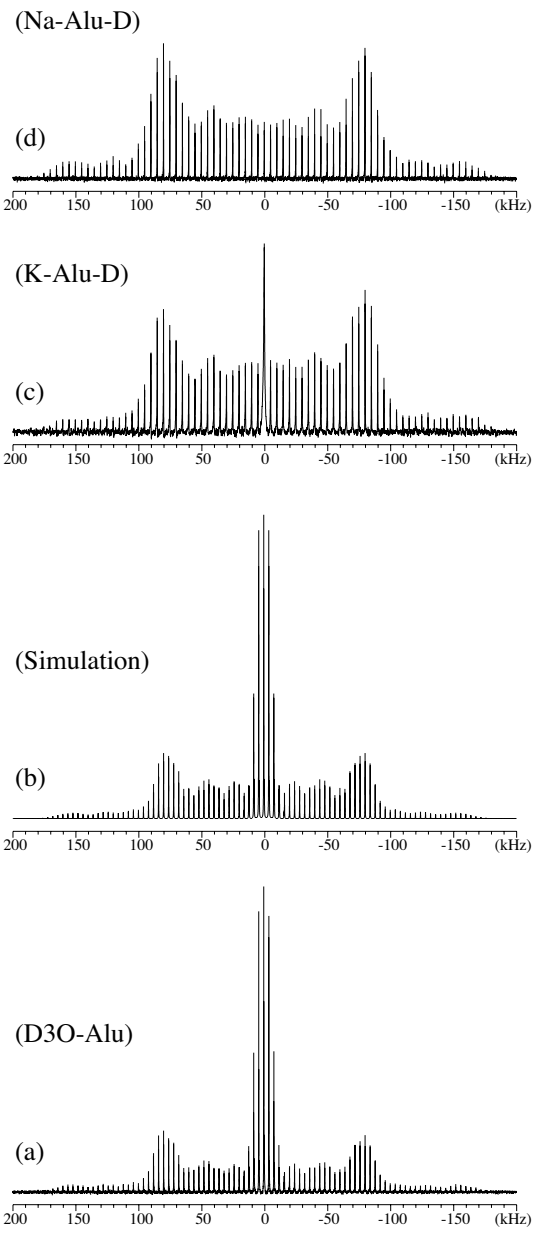

FIGURE 6. ^{2}H MAS NMR spectra of deuterated sample (**a**) D_3O-Alu (4 kHz), (**c**) K-Alu-D (5 kHz), and (**d**) Na-Alu-D (5 kHz). (**b**) A simulation of D_3O-Alu using $\delta_{iso} = 4.0$ ppm, $C_Q = 235$ kHz, $\eta_Q = 0.02$ for OD and $\delta_{iso} = 10.3$ ppm, $C_Q = 17$ kHz, $\eta_Q = 0.45$ with a relative intensity of 2:1 for the OD and D_3O^+ sites.

constants and O-H···O distances by Poplett and Smith (1978), a O-H···O distance of 2.86(5) Å is obtained implying rather weak hydrogen bonding. Alunite minerals contain a weak hydrogen bond between the Al_2-OH group and the unique O atom in the sulfate group pointing into the cavity. Although no satisfactory structural model is available for a pure D_3O^+ alunite, a direct comparison with alunite [$KAl_3(SO_4)_2(OH)_6$] is possible since these structures have similar unit-cell parameters. An O-H···O distance of 2.91 Å (Schukow et al. 1999) was obtained for an alunite sample with nominally 12% H_3O, which is in excellent agreement with our measurement.

The width of the ssb pattern for the second site with δ_{iso} = 10.1 ppm is significantly narrower and has a much smaller ^{2}H quadrupole coupling caused by rapid molecular motions of the deuterons on this site. Least-squares optimization to the integrated ssb intensities gave $C_Q = 17(5)$ kHz. The optimizations are less sensitive to the variations of the asymmetry parameter due to the weak quadrupole interaction. A best shallow best-fit minimum is observed for $\eta_Q \approx 0.45$, which also reproduces the intensity of the ssbs manifold from D_3O^+ in the simulations. Characteristic values for the quadrupole tensor are observed for various types of motion. For example, -OD_2 groups with rapid C_2 motion are characterized by $C_Q \approx 70$ kHz and $\eta_Q = 1$ (Soda and Chiba 1969; Spiess and Sillescu 1981) and a D_3O^+ ion rotating about its C_3 axis results in $C_Q \approx 70$ kHz and $\eta_Q = 0.00$ (1/3 of the full tensor). Thus, the much smaller value determined here (C_Q = 17 kHz) reflects a more complex motional averaging involving rotation around more than one axis, but that is less than complete isotropic motion. Ripmeester et al. (1986) estimated a C_Q of approximately 24 kHz for a model with twelve-site averaging. A much weaker resonance due to a third site with $\delta_{iso} = 5.9(3)$ ppm is visible in the isotropic region, but absence of ssbs prevented further analysis.

Excellent agreement is observed between the full experimental spectrum and a simulation performed using the parameters for the two main sites discussed above, when a relative intensity of 1:0.53(5) for OD:D_3O^+ is employed (Figs. 6a and 6b). The relative intensity is in excellent agreement with the 1:0.5 ratio expected from the crystal structures confirming the complete occupancy of the *A* site by the D_3O^+ ion in this synthetic sample. It should be emphasized that our ^{1}H and ^{2}H MAS NMR studies were performed on two samples with *different* concentrations of defects (Table 1). Normalized to the sulfate, elemental analysis of deuterated hydronium alunite suggest that the sample is near-stoichiometric $(D_3O)\ Al_{3.01}\ (SO_4)_2\ (OD)_{6.}$, (within experimental uncertainties) whereas the protonated sample has the composition: $(H_3O)Al_{2.83}(SO_4)_2(OH)_{5.49}(H_2O)_{0.51}$, (Table 1). The calculation of the H/D contents assumes full occupancy on the A^+ site, which may not be a correct assumption (Majzlan et al. 2004).

The ^{1}H MAS NMR spectrum of D_3O-Alu (not shown) contains the same resonances as seen for H_3O-Alu. Additional fine structure is observed in ^{1}H MAS NMR spectrum of the deuterated hydronium alunite, and three different peaks, at 10.1, 11.0 (ca. 90% of the intensity), and 11.5 ppm are partly resolved. ^{1}H MAS NMR spectra recorded at 16.4 T (700 MHz) shows that the peak position is independent of the magnetic field strength. Thus, the three resonances originate from slightly different local environments and are not due to fine structure caused by, e.g., J-coupling or second order effects. This splitting may originate from slightly different local environments. The increased resolution for the deuterated sample is due to a reduction by isotope dilution of the strong homo-nuclear ^{1}H dipolar coupling, which cannot be fully averaged by MAS at these moderate spinning speeds. No additional resonances are seen (apart from the weak resonance at 5.3 ppm), further confirming that this D_3O-Alu sample contains few defects.

Synthetic alunite (K-Alu and K-Alu-D). The ^{1}H spectrum of K-Alu (Fig. 5b) shows two peaks, the Al_2-OH group at δ_{iso} =

3.9 ppm and a resonance at δ_{iso} = 6.4 ppm with relative intensities of 1:0.53. The very intense 6.4 ppm resonance suggests the presence of a significant amount of Al^{3+} vacancies in this compound, assuming that assignment of this resonance to Al-OH_2 groups is correct. The signal from the hydronium ion (δ_{iso} = 10.6 ppm) observed in H_3O-Alu is not visible in the ^{1}H MAS NMR spectrum.

The ^{2}H MAS NMR spectrum (Fig. 6c) of a partially deuterated sample, K-Alu-D, prepared in a similar manner to K-Alu, contains two resonances. The first is assigned to the Al_2-OD groups and has values of δ_{iso} = 4.0(5), C_Q = 237(5) kHz, and η_Q = 0.07(5), as obtained from least-squares optimization to the integrated ssb intensities. An O-H···O distance of 2.87(5) Å is obtained using the correlation between C_Q and $r_{O-H---O}$ (Poplett and Smith 1978). A single, intense peak with a broad Lorentzian line shape [full-width, half-maximum (FWHM) = 800 Hz] centered near δ = 7.0 (1.5) ppm is also observed with no associated ssbs. The lack of ssbs implies chemical exchange and/or isotropic rotation on the time scale of the quadrupole coupling for this resonance. The characteristic ssb pattern expected for an Al-OH_2 group undergoing rapid flips around the C_2 axis is not observed. One possibility is that the Al-OD_2 groups are strongly hydrogen-bonded and therefore rigid; in this case, since the chemical shift difference between the Al_2-OD and Al-OD_2 groups is small in comparison to the ssb linewidth, the signal due to the Al-OD_2 group cannot be resolved from the Al_2-OD resonance. Very slow motion, on a timescale governed by both C_Q and the spinning speed, can also prevent refocusing of the signal and may result in the loss of the Al-OD_2 resonance. The observed signal at 7.0 ppm is then assigned to the Al-OD_2 groups that are undergoing more rapid motion. Static ^{2}H NMR spectra (not shown) were acquired to distinguish between these possibilities. A line shape was observed which could be deconvoluted into a broader Pake doublet due to rigid OD groups, and a sharper intense component due to mobile deuterons. Thus, the Al-OD_2 groups are most likely absent in the MAS spectra due to short T_2^*s (effective transverse relaxation times); this will be discussed in more detail below.

Natroalunite (Na-Alu and Na-Alu-D). The ^{1}H MAS NMR spectrum contains two resonances, at δ_{iso} = 4.9 ppm (Al_2-OH) and at δ_{iso} = 7.9 ppm with a relative ratio of 1:0.09 (Fig. 5c and Table 3). Both peaks are shifted approximately 1 ppm compared to alunite and hydronium alunite (Table 3). Similar to K-Alu, no H_3O^+ resonance is observed. The intensity of the Al-OH_2 peak is much smaller than expected based on both the elemental analysis and the ^{27}Al NMR, where Al_D sites were clearly observed. ^{2}H MAS NMR spectra (Fig. 6d) of a deuterated sample can be simulated with a single Al_2-OD site characterized by δ_{iso} = 4.0(9) ppm, C_Q = 240(5) kHz, η_Q = 0.09(8), as obtained from least-squares optimization to the integrated ssb intensities. This corresponds to a O-H···O distance of 2.89(5) Å (Poplett and Smith 1978) and is in agreement with the value determined from XRD [2.86(1) Å] (Okada et al. 1982). No other peaks can be observed in the ^{2}H MAS NMR spectra. The ^{1}H MAS NMR spectra (not shown) of this per-deuterated sample show the presence of two peaks, Al_2-OH (δ_{iso} = 4.3 ppm) and a weaker Al-OH_2 resonance (δ_{iso} = 7.5 ppm), similar to those observed for Na-Alu. Again, both the ^{2}H and ^{1}H NMR results suggest that slow motion involving the Al-OH_2 groups is occurring, which may distort the intensities seen in the echo spectra (^{1}H).

TABLE 3. ^{1}H chemical shifts (δ_{iso}) and relative intensity for the alunites determined from deconvolution of ^{1}H MAS NMR spectra recorded at 14.1 T [υ_L (^{1}H) = 600.1 MHz]

Compound	Group	δ_{iso} (ppm)	Intensity*	Concentration†
K-Alu	Al-OH	3.9 ± 0.3	65 ± 3	78 ± 3%
	Al-OH_2	6.4 ± 0.3	35 ± 3	21 ± 3%
Na-Alu	Al-OH	4.9 ± 0.3	93 ± 3	≈ 95%
	Al-OH_2	7.9 ± 0.3	8 ± 5	<5%
H_3O-Alu	Al-OH	4.0 ± 0.3	48 ± 3	73 ± 4%
	Al-OH_2	6.2 ± 0.5	13 ± 4	
	–	9.5 ± 0.5	4 ± 3	≈ 5%‡
	H_3O^+	10.6 ± 0.5	35 ± 3	18 ± 4%
Nat-Alu	Al-OH	3.9 ± 0.3	92 ± 5	≈ 95%
	Al-OH_2	6.7 ± 0.5	5 ± 4	≈ 3%
	Other	5.2 ± 0.5	4 ± 4	≈ 3%

Notes: Spectral intensities are obtained from deconvolution of the isotropic region as well as the spinning side bands from echo-experiments. The experiments have not been corrected for variations in T_2.
* This relates to the total integrated intensity of the peak.
† The relative intensity of each functional group corrected for the spin multiplicity as needed and normalized.
‡ Total intensity of the two resonances.

Natural Alunite (Nat-Alu). The ^{1}H MAS NMR spectrum of this sample (Fig. 5d) shows a broad resonance with $\delta_{iso} \approx 4$ ppm with approximately 95% of the total spectral intensity. Within uncertainty the isotropic chemical shift is identical to that for the Al_2-OH/H_2O group in synthetic K-Alu. Two peaks in the region for Al-OH_2 and H_2O with δ_{iso} = 5.2 and 6.7 ppm, respectively, are obtained from a fit of the ^{1}H MAS NMR spectrum, as illustrated in Figure 5d. The resonance at δ_{iso} = 5.2 ppm is assigned to an unknown impurity or defect. These results are consistent with the ^{27}Al data, which suggest the presence of very few defects.

Slow-speed ^{1}H MAS NMR spectra. Single-pulse ^{1}H MAS NMR spectra were recorded using a low proton background probe. These spectra show the same resonances as seen in the ^{1}H MAS Hahn-echo experiments (Fig. 5); this is illustrated in Figure 7 for selected alunite samples. Both the Al_2-OH and Al-OH_2 resonances have several intense ssbs indicating strong ^{1}H-^{1}H (and ^{1}H-^{27}Al) dipolar coupling. For all samples, the Al-OH_2 resonance is more intense in the single-pulse spectra than in the echo-experiments, implying that this system is strongly coupled and that different relaxation times (T_2) probably affects the data obtained in the echo-experiment. The intensity is quite similar to that of the Al_2-OH resonance (Fig. 7b). For Na-Alu, ca. 90% of the intensity in the center band is from Al_2-OH and ca. 10% Al-OH_2 based on fitting to the center band only, higher than observed in the echo-experiment. However, precise quantification of these slow speed single-pulse ^{1}H MAS NMR spectra proved difficult and unambiguous solutions to the fits could not be obtained, because of complicated centerband and ssb peak shapes owing to a combination of chemical shifts anisotropy (CSA) and dipolar coupling.

^{27}Al {^{1}H} HETCOR NMR

H_3O-Alu. HETCOR is a 2-dimensional NMR experiment, which gives cross-peaks between protons and aluminum that are in a close spatial proximity. We note that these spectra are not necessarily quantitative, due to variations in CP efficiency. The ^{27}Al {^{1}H} HETCOR spectrum of H_3O-Alu shows the presence of two cross-peaks. The more intense is centered at $\delta(^1H) \approx 5$ ppm and the second at $\delta(^1H) \approx 10$ ppm (Fig. 8). The two cross-peaks

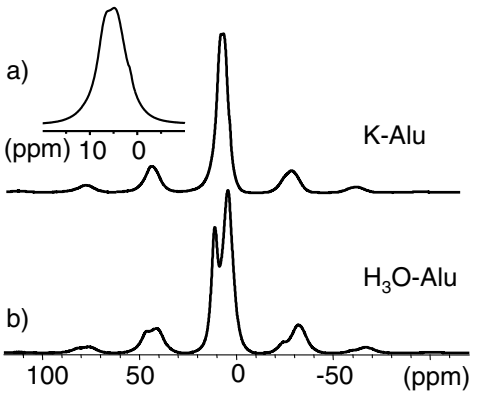

FIGURE 7. Single-pulse ^{1}H MAS NMR spectra of (**a**) K-Alu and (**b**) H_3O-Alu at 400 MHz (9.4 T) using 14 kHz spinning speed. Spectra were recorded using a probe with a negligible ^{1}H background.

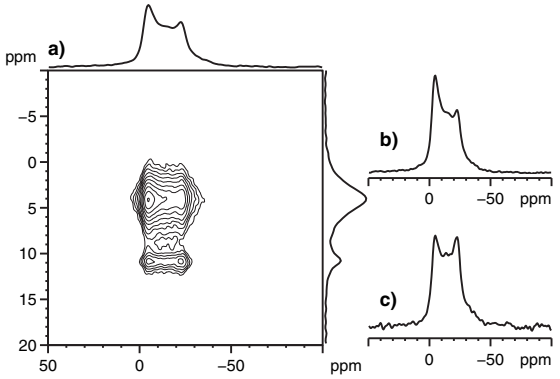

FIGURE 8. (**a**) ^{1}H, ^{27}Al HETCOR NMR spectra of H_3O-Alu at 14.1 T obtained by using a 100 µs contact time and 14 kHz spinning speed. Summed slices projected on to the ^{27}Al dimension are shown for (**b**) the Al-OH resonance and (**c**) the H_3O^+ resonance.

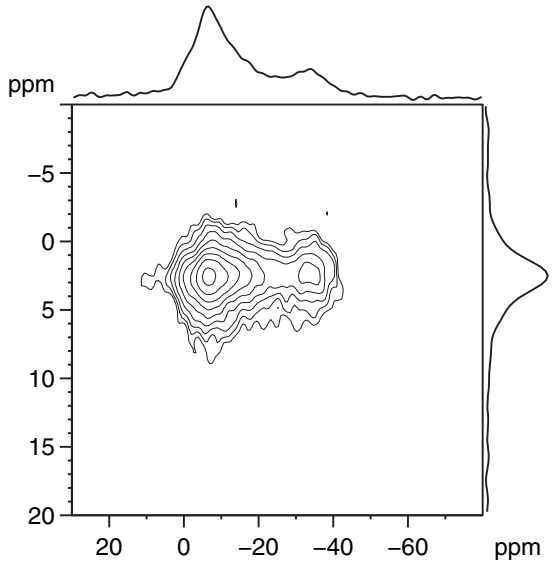

FIGURE 9. ^{1}H, ^{27}Al HETCOR NMR spectra of K-Alu and at 14.1 T using the same condition as in Figure 8.

show quite different ^{27}Al line shapes, the $\delta(^{1}H) \approx 10$ ppm cross-peak resembling that of the Al1 environment, the $\delta(^{1}H) \approx 5$ ppm cross-peak showing much more intensity at lower frequency and more closely resembling the ^{27}Al spectra of Na-Alu and K-Alu. The line shape of the 5 ppm cross-peak is consistent with the presence of resonance(s) from one or more defects, in addition to the resonance due to Al1. These defect resonances may be enhanced in the HETCOR spectrum, because the smaller values of C_Q for these environments, in comparison to the C_Q value of Al1, result in their more efficient cross-polarization.

K-Alu. The ^{27}Al $\{^{1}H\}$ HETCOR spectrum of K-Alu (Fig. 9) shows the presence of a single, broad cross-peak with a center of gravity at $\delta(^{1}H) \approx 5$ ppm and a cross-section in the ^{27}Al dimension gives a line shape with the same features as seen in the ^{27}Al MAS NMR spectrum of K-Alu. Thus, ^{27}Al $\{^{1}H\}$ HETCOR experiments confirm that all four ^{27}Al resonances are linked to the protons (Fig. 3d). Unfortunately, the resolution in the proton dimension is lower than in single-pulse ^{1}H MAS NMR experiments, and it was not possible to resolve the Al_2-OH and Al-OH_2 resonances with the spinning frequencies used in these experiments. The efficient cross-polarization observed for Al-OH_2 groups suggest that these are fairly rigid. A similar spectrum was obtained for Na-Alu (not shown).

^{39}K MAS NMR

To obtain further information about the local structure, ^{39}K MAS NMR were recorded of K-Alu and K-Alu-D; spectra were not recorded for Nat-Alu due to a limited amount of the sample. The experimental ^{39}K MAS NMR spectrum of K-Alu (Fig. 10a) exhibits a well-defined high-frequency singularity and then slowly tails off. This line shape is characteristic of a distribution of ^{39}K quadrupole coupling constants. A good fit to the experimental spectrum has been obtained with a Gaussian distribution of the EFG tensor centered at $C_Q = 1.7$ MHz with a FWHM of 0.7 MHz and $\delta_{iso} \approx 2$ ppm using the method of Coster et al. (1994). For K-Alu-D, $C_Q = 1.8$ MHz (FWHM = 0.6 MHz), $\delta_{iso} \approx 0$ ppm, which is identical within the error-limits of those determined for K-Alu. We note that the calculations of the second-order quadrupolar line shape assume $\upsilon_r >> \upsilon_{2Q}$. This is not fulfilled for the experimental spectra due to the limited spinning speed of the 5 mm MAS probe, resulting in small deviations between the experimental and simulated line shapes.

The value of C_Q and the chemical shift is consistent with reports for other inorganic materials (Bastow 1991; Smith 2000; Stebbins et al. 2002). The ^{39}K quadrupole coupling is sensitive to ions in the first and second coordination sphere (Koller et al. 1994). Each potassium ion is coordinated by 12 O atoms of which six are the bridging Al_2-OH groups. Thus, 6 Al atoms are located in the first cation coordination sphere (Fig. 1). The ca. 10% Al vacancies in this sample inferred from the ^{27}Al NMR implies that a large fraction (>50%) of K has at least one Al vacancy in the second coordination sphere accounting for the distribution of quadrupole couplings.

^{23}Na MAS NMR of Na-Alu

The ^{23}Na 3QMAS NMR spectrum (Fig. 11) reveals a single resonance with a distribution of both the chemical shift and quadrupole coupling. Sodium is located on a site with $\bar{3}m$ point group symmetry implying an axially symmetric ^{23}Na quadru-

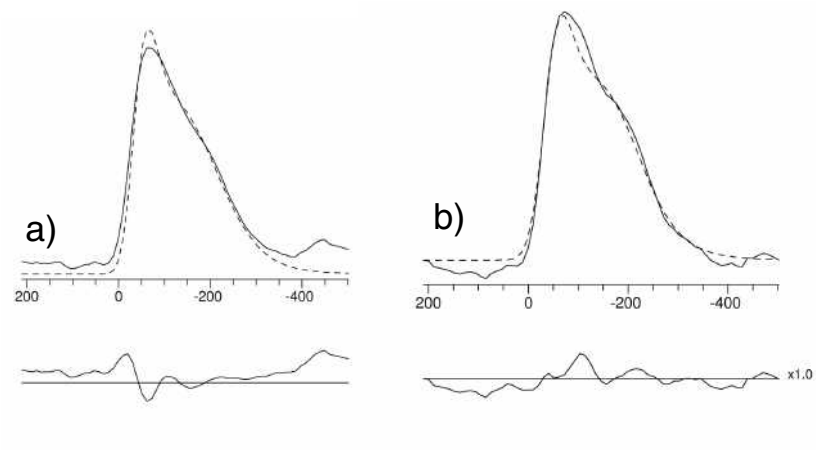

FIGURE 10. ^{39}K MAS NMR spectra of (**a**) K-Alu (solid line) with a simulation (---) using a distribution of the quadrupole coupling of 0.7 MHz centered at 1.7 MHz. (**b**) K-Alu-D (solid line) and simulation (---) of a C_Q distribution of 0.6 MHz with C_Q = 1.8 MHz. Experimental spectra were recorded at 11.7 T (23.3 MHz) employing a spinning speed of 9 kHz. The difference between the experimental and simulated is shown below.

pole tensor (η_Q = 0). $\delta_{iso} \approx -22$ ppm and C_Q is estimated to be 1.3 (± 0.3) MHz is estimated from the 3QMAS NMR spectrum assuming η_Q = 0.

DISCUSSION

^{27}Al defect resonances and interpretation of quadrupolar parameters. Al1 and Al_D represent most of the total intensity (> 90%) in the ^{27}Al MAS NMR spectra of all samples studied. For example, using the ^{27}Al NMR parameters listed in Table 2, the following composition is obtained from a fit of the spectrum of K-Alu (Fig. 3d): 60(5)% originates from Al1, 35(5)% from Al_D, and approximately 2–4% each from Al_{I1} and Al_{I2}. For each sample, the intensity of the Al_D ^{27}Al resonance is closely correlated with (1) the appearance of the Al-OH_2 resonance in the ^{1}H NMR spectrum of the same sample and (2) the abundance of Al vacancies according to the elemental analyses. This correlation supports our assignment of the Al_D resonance to an aluminum site adjacent to an Al vacancy (Fig. 2). Assignments for the Al_{I1} and Al_{I2} resonances are uncertain. They could arise from Al1 sites in alunite with more than one adjacent Al vacancy or from impurities not detected by XRD. Solid-state NMR spectroscopy is often more sensitive to small concentrations of impurities than routine XRD, e.g. (Nielsen et al. 2002). The ^{27}Al NMR parameters determined for Al_{I1} and Al_{I2} in K-Alu and Al_I in Na-Alu are typical values observed for sulfate phases containing the hexaqua ion ($Al(H_2O)_6$) (Phillips and Feng, unpublished) or small hydrated Al oligomers. These phases are very difficult to detect as they may be present below the detection limit of powder XRD (2–3%) or may be amorphous. Such impurities could have a different stoichiometry than alunite, and could skew the elemental analyses data, which determines the overall, bulk composition of the sample.

We can estimate the concentration of Al vacancies in alunite and hence the Al site occupancy from the equation

$$Al1 + Al_D + \square = I(Al1) + 5/4I(Al_D) = 100\% \quad (3)$$

This equation assumes that the vacancies are isolated and that Al_{I1}, Al_{I2}, and Al_I arise from impurities. Using this assumption, each isolated vacancy (□) generates four Al_D sites, cf. Figure 2. A 92(5)% occupancy of Al site is obtained for K-Alu using this method. The Al occupancy of other synthetic alunite and natroalunite samples (K-Alu-D, Na-Alu, and Na-Alu-D) are also around 90(6)%. Thus, even a few percent of Al vacancies results in a significant concentration of the Al_D site, which can be readily detected by ^{27}Al NMR spectroscopy. Removal of more Al ions in the second coordination sphere is expected to create additional resonances, which we predict to have smaller quadrupole couplings. These may not be observed in the ^{27}Al 3QMAS NMR spectra or may be responsible for all or some of the resonances assigned to impurities.

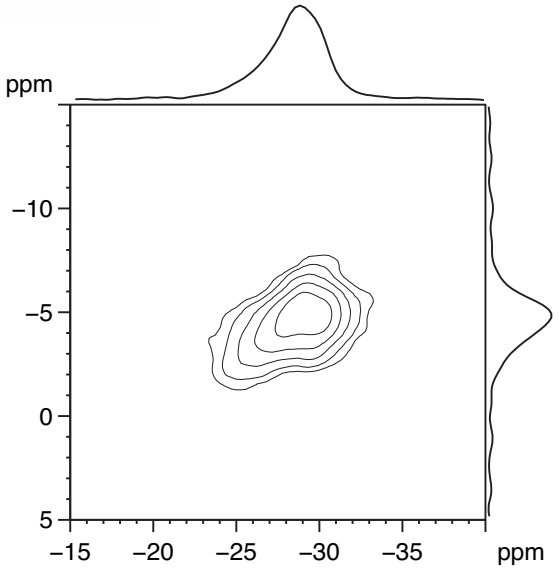

FIGURE 11. ^{23}Na 3QMAS NMR spectra of Na-Alu recorded at 14.1 T (158.3 MHz) employing a spinning speed of 14 kHz.

Quadrupole couplings are very sensitive to the local bonding environment especially first and second coordination spheres. For ^{27}Al correlations between longitudinal strain for C_Q(^{27}Al) and octahedrally coordinated Al have been established (Ghose and Tsang 1973). The aluminum octahedron in the perfect alunite structure has a large variation in Al-O bond lengths between the axial and equatorial bonds of 1.864 and 1.951 Å, respectively (Wang et al. 1965). This difference results in a significant longitudinal strain (α) of 0.14 for alunite ($\alpha = \sum \left| \ln(l_i / l_0) \right|$), where l_i is the actual Al-O bond length, and l_0 is the ideal bond length

in a perfect octahedron of the same total volume (Ghose and Tsang 1973). The observation of very large ^{27}Al C_Q's of 8.6 and 10.5 MHz for the Al1 in hydronium alunite and alunite are in excellent agreement with $\alpha = 0.14$. The large difference in the size of the ^{27}Al C_Q between the two alunite samples is ascribed to the presence of different cations in the second coordination sphere and the small differences in lattice parameters. Removing an Al^{3+} in the second coordination sphere destroys the approximately fourfold symmetry at the Al site and relaxes the Al-O bond lengths and angles to accommodate the addition of a proton. Specifically, the Al-O distances are typically longer for Al-OH_2 (ca. 1.9 Å) compared to bridging Al_2-OH (1.86 Å) (Schukow et al. 1999). Substitution of terminal OH_2 ligands for bridging hydroxyls results in a smaller quadrupole coupling and a non-axially symmetric local ^{27}Al-bonding environment, as observed for Al_D (Table 2).

The distribution of the quadrupole couplings in the less defective natural alunites and synthetic hydronium alunites is ascribed to small structural variations caused by distant Al defects propagating through the structure or *A*-site vacancies. The presence of Al vacancies (and impurities) is readily confirmed by ^{27}Al MAS and 3QMAS NMR spectroscopy via the observation of new ^{27}Al NMR resonances.

Defect ^1H NMR resonances and alunite stoichiometry

The sample compositions derived from ^1H and ^2H NMR and elemental analysis, based on the convention for the compensation of Al-vacancies and *A*-site defects by protons, do not agree very well. Furthermore, inconsistency between ^1H and ^2H NMR data suggest some loss of signal intensity in the ^1H MAS echo and ^2H MAS owing to strong homo-nuclear (^1H-^1H) dipolar couplings or molecular motion on the order of the NMR time scale. The ^2H MAS NMR spectra can be strongly effected by motion on the timescale governed by $t/\tau_c \approx (C_Q/\nu_r)^2$ (Maricq and Waugh 1979) where ν_r is the spinning frequency and τ_c the motional correlation time. This effect can cause a significant broadening and even disappearance of the resonances in the limit of very slow motion. A distinct resonance that could be assigned to the Al-OD_2 group was not observed in the ^2H MAS spectra of samples that clearly contain Al vacancies on the basis of elemental analysis and ^{27}Al NMR. This result suggests that the Al-OH_2 groups are either (1) rigid, not undergoing C_2 flipping motions, or (2) exhibit slow molecular motion that broadens the ssbs beyond detection. The static ^2H NMR results for alunite suggest that the second hypothesis is correct.

No H_3O^+ resonance is observed in any of the alunite and natroalunite samples investigated. On this basis, we estimate that the occupancy of H_3O^+ at the *A* site is less than 2% in these samples. Elemental analysis combined with the assumption of 100% *A*-site occupancy, however, suggests ca. 21% occupancy of H_3O^+ in the K-Alu and a stoichiometry $K_{0.79}(H_3O)_{0.21}Al_{2.49}(SO_4)_2(OH)_{4.47}(H_2O)_{1.53}$. For Na-Alu, a composition of $Na_{0.83}(H_3O)_{0.17}Al_{2.28}(SO_4)_2(OD)_{5.49}(H_2O)_{2.16}$ is obtained from elemental analysis. The lack of an H_3O^+ resonance suggests that the H_3O^+ ions are found nearby the Al vacancies so that the fourth Al-OH group at the vacancy is charge compensated by the H^+ of the H_3O^+ ion, as outlined in reaction 2. This would result in 4 Al-OH_2 groups and a H_2O molecule, which is consistent with the observed ^1H shift of 6.4 ppm for the "defect" resonance and the absence of a H_3O^+ resonance. Given the stoichiometry $(K_{0.79})(H_3O)_y Al_{2.49}\square_{0.51}(SO_4)_2(OH_2)_x(OH)_{6-x}$ for K-Alu based solely on the elemental analysis, where we have made no assumption as to the mechanism for compensation of *A*- and *B*-site vacancies, Equation 1 predicts that x = 1.53 (3 × 0.51), while Equation 2 predicts that x = 2.04. Given the number of K^+ per formula unit (pfu, 0.79), no more than 0.21 H^+ ions pfu may be present. Hence x is constrained to a maximum value of x = 1.75, assuming all the H^+ ions are bound to the Al-OH groups of the defect. In this case, the *A* site contains between 0.21 and zero water molecules. In this limit a ratio of the concentration of the Al_2-OH:Al-OH_2 groups of 4.25:1.75 is predicted, and ^1H intensities of 4.25:3.5. Any water present in the *A* site will contribute to the Al-OH_2 resonance. The Al_2-OH and Al-OH_2 peaks are of approximately equal intensity in the one-pulse spectra (Fig. 7a) supporting the substitution mechanism of Equation 2. The lower concentration of the Al-OH_2 resonance in the echo-spectrum is ascribed to problems associated with different T_2 relaxation in the echo experiment. Rigid Al-OH_2 groups clustered at the vacancy would exhibit strong ^1H-^1H homonuclear coupling and these short spin-spin relaxation times (T_2) would result in a reduced intensity relative to the more weakly coupled Al_2-OH sites in spectra obtained by echo methods. The discrepancy is more severe for natroalunite, where the Al-OH_2 peak in the ^1H MAS NMR echo and one-pulse spectra is not intense enough to account for the number of defects according to a similar analysis of the sample stoichiometry. It is also possible to speculate that intensity is lost due to slow exchange of the protons among the larger number of structural defects. Moreover, slow motion may not only involve the Al-OH_2 groups, but also the Al-OH groups present in this much more defective sample. This may account for the noticeable shift of the Al_2-OH resonance from 3.9 ppm in K-Alu to 4.9 ppm in Na-Alu. Thus, care should be taken when interpreting the quantitative analysis of ^1H MAS NMR spectra of defect alunite samples. Further variable temperature ^1H and ^2H NMR studies are needed to fully understand the complex proton system in defect alunite samples, but is beyond the scope of this paper.

Finally, the results for the alunite and natroalunite samples suggests that the discrete H_3O^+ resonance observed in H_3O-Alu at 10.6 ppm may arise from the stoichiometric regions in the sample, where the H_3O^+ ions are far from Al vacancies. This conclusion is further supported by the ^{27}Al {^1H} HETCOR NMR experiments, which show that H_3O^+ ions are near only Al1 sites. Thus, reaction 2 takes place in defect alunite samples and the existence of the H_3O^+ ion and the absence of vacancies on the *A* site is closely linked to the stoichiometry of *B* site in alunite. It is likely that similar defect compensation mechanisms occur in non-stoichiometric jarosites and experiments are currently in progress to test this hypothesis.

Acknowledgments

U.G.N. acknowledges the "Camille and Henry Dreyfus Postdoctoral Program in Environmental Chemistry" and Carlsbergfondet (ANS-1323/20) for financial support. J.M. appreciates the support that came from the Hess post-doctoral fellowship at the Department of Geosciences at Princeton University. We thank S. Hirth-Walther for help with the chemical analyses of the alunite samples. This work was supported by NSF-grants CHE-0221934 to fund the Center for Environmental Molecular Science and CHE-03-21001 for instrumentation.

REFERENCES CITED

Akitt, J.W. and Elders, J.M. (1988) Multinuclear magnetic resonance studies of the hydrolysis of Aluminium(III). Part 9. Base hydrolysis monitored at very high magnetic field. Journal of the Chemical Society—Dalton Transactions, 10, 1347–1355.

Amoureux, J.-P., Fernandez, C., and Frydman, L. (1996) Optimized multiple-quantum magic-angle spinning NMR experiments on half-integer quadrupoles. Chemical Physics Letters, 259, 347–355.

Bastow, T.J. (1991) Powder determination of ^{39}K nuclear quadrupole coupling. Journal of the Chemical Society—Faraday Transactions, 87, 2453–2455.

Bennett, A.E., Rienstra, C.M., Auger, M., Lakshmi, K.V., and Griffin, R.G. (1995) Heteronuclear Decoupling in Rotating Solids. Journal of Chemical Physics, 103, 6951–6958.

Berglund, B. and Vaughan, R.W. (1980) Correlations between proton chemical shift tensors, deuterium quadrupole couplings, and bond distances for hydrogen bonds in solids. The Journal of Chemical Physics, 73, 2037–2043.

Bishop, J.L. and Murad, E. (2005) The visible and infrared spectral properties of jarosite and alunite. American Mineralogist, 90, 1100–1107.

Bohmhammel, K., Brand, P., and Härtig, C. (1986) Zur Existenz der Oxoniumionen in festen basichen Aluminiumsulfaten. Zeitschrift für Anorganische und Allgemeine Chemie, 542, 201–206.

Coster, D., Blumenfeld, A.L., and Fripiat, J.J. (1994) Lewis-acid sites and surface aluminum in aluminas and zeolites—a high-resolution NMR-study. Journal of Physical Chemistry, 98, 6201–6211.

Drouet, C. and Navrotsky, A. (2003) Synthesis, characterization, and thermochemistry of K-Na-H_3O jarosites. Geochimica et Cosmochimica Acta, 67, 2063–2076.

Drouet, C., Pass, K.L., Baron, D., Draucker, S., and Navrotsky, A. (2004) Thermochemistry of jarosite-alunite and natrojarosite-natroalunite solid solutions. Geochimica et Cosmochimica Acta, 68, 2197–2205.

Dutrizac, J.E. and Jambor, J.L. (2000) Jarosites and their application in hydrometallurgy. In C.N. Alpers, J.L. Jambor, and D.K. Nordstrom, Eds., Sulfate Minerals—Crystallography, Geochemistry and Environmental Significance, 40, p. 405–452. Reviews in Mineralogy and Geochemistry, Mineralogical Society of America, Chantilly, Virginia.

Frydman, L. and Harwood, J.S. (1995) Isotropic spectra of half-integer quadrupolar spins from bidimensional magic-angle spinning NMR. Journal of the American Chemical Society, 117, 5367–5368.

Ghose, S. and Tsang, T. (1973) Structural dependence of quadrupole coupling constant e^2qQ/h for ^{27}Al and crystal field parameter D for Fe^{3+} in aluminosilicates. American Mineralogist, 58, 748–755.

Greedan, J.E. (2001) Geometrically frustrated magnetic materials. Journal of Materials Chemistry, 11, 37–53.

Grohol, D. and Nocera, D.G. (2002) Hydrothermal oxidation-reduction methods for the preparation of pure and single crystalline alunites: Synthesis and characterization of a new series of vanadium jarosites. Journal of the American Chemical Society, 124, 2640–2646.

Grohol, D., Nocera, D.G., and Papoutsakis, D. (2003) Magnetism of pure iron jarosites. Physical Review B (Condensed Matter and Materials Physics), 67, 064401.

Harrison, A. (2004) First catch your hare*: the design and synthesis of frustrated magnets. Journal of Physics—Condensed Matter, 16, S553–S572.

Jansen, S.R., Hintzen, H.T., Metselaar, R., de Haan, J.W., van de Ven, L.J.M., Kentgens, A.P.M., and Nachtegaal, G.H. (1998) Multiple quantum Al-27 magic-angle-spinning nuclear magnetic resonance spectroscopic study of $SrAl_{12}O_{19}$: Identification of a Al-27 resonance from a well-defined AlO_5 site. Journal of Physical Chemistry B, 102, 5969–5976.

Klingelhöfer, G., Morris, R.V., Bernhardt, B., Schröder, C., Rodionov, D.S., de Souza, P.A., Jr., Yen, A., Gellert, R., Evlanov, E.N., Zubkov, B., Foh, J., Bonnes, U., Kankeleit, E., Gutlich, P., Ming, D.W., Renz, F., Wdowiak, T., Squyres, S.W., and Arvidson, R.E. (2004) Jarosite and Hematite at Meridiani Planum from Opportunity's Mössbauer Spectrometer. Science, 306(5702), 1740–1745.

Koller, H., Engelhardt, G., Kentgens, A.P.M., and Sauer, J. (1994) Na-23 NMR-spectroscopy of solids—Interpretation of quadrupole interaction parameters and chemical-shifts. Journal of Physical Chemistry, 98, 1544–1551.

Kurata, M., Kaneko, K., and Inouye, K. (1984) Preparation of porous alunite and its water adsorption. Journal of Physical Chemistry, 88, 2119–2124.

Kydon, D.W., Pintar, M., and Petch, H.E. (1968) NMR evidence of H_3O^+ ions in gallium sulfate. Journal of Chemical Physics, 48, 5348–5351.

Lager, G.A., Swayze, G.A., Loong, C.-K., Rotella, F.J., Richardson, J.W., and Stoffregen, R.E. (2001) Neutron spectroscopic study of synthetic alunite and oxonium-substituted alunite. Canadian Mineralogist, 39, 1131–1138.

Larson, A.C. and von Dreele, R.B. (1994) GSAS. General Structure Analysis System, LANSCE, MS-H805, Los Alamos, New Mexico.

Madden, M.E.E., Bodnar, R.J., and Rimstidt, J.D. (2004) Jarosite as an indicator of water-limited chemical weathering on Mars. Nature, 431(7010), 821–823.

Majzlan, J., Stevens, R., Boerio-Goates, J., Woodfield, B.F., Navrotsky, A., Burns, P.C., Crawford, M.K., and Amos, T.G. (2004) Thermodynamic properties, low-temperature heat-capacity anomalies, and single-crystal X-ray refinement of hydronium jarosite, $(H_3O)Fe_3(SO_4)_2(OH)_6$. Physics and Chemistry of Minerals, 31, 518–531.

Maricq, M.M. and Waugh, J.S. (1979) NMR in rotating solids. The Journal of Chemical Physics, 70, 3300–3316.

Massiot, D., Touzo, B., Trumeau, D., Coutures, J.P., Virlet, J., Florian, P., and Grandinetti, P.J. (1996) Two-dimensional magic-angle spinning isotropic reconstruction sequences for quadrupolar nuclei. Solid State Nuclear Magnetic Resonance, 6, 73–83.

Massiot, D., Franck, F., Mickael, C., King, I., Le Calvé, S., Alonso, B., Durand, J.-O., Bujoli, B., Gan, Z., and Hoatson, G. (2002) Modelling one- and two-dimensional solid-state NMR spectra. Magnetic Resonance in Chemistry, 40, 70–76.

Müller, D., Gessner, W., Behrens, H.J., and Scheler, G. (1981) Determination of the aluminum coordination in aluminum-oxygen compounds by solid-state high-resolution Al-27 NMR. Chemical Physics Letters, 79, 59–62.

Nielsen, U.G., Boisen, A., Brorson, M., Jacobsen, C.J.H., Jakobsen, H.J., and Skibsted, J. (2002) Aluminum orthovanadate ($AlVO_4$): Synthesis and characterization by ^{27}Al and ^{51}V MAS and MQMAS NMR spectroscopy. Inorganic Chemistry, 41, 6432–6439.

Nocera, D.G., Bartlett, B.M., Grohol, D., Papoutsakis, D., and Shores, M.P. (2004) Spin frustration in 2D kagome lattices: A problem for inorganic synthetic chemistry. Chemistry—a European Journal, 10, 3851–3859.

Okada, K., Hirabayashi, J., and Ossaka, J. (1982) Crystal-structure of natroalunite and crystal-chemistry of the alunite group. Neues Jahrbuch für Mineralogie-Monatshefte, 534–540.

Ozeki, S., Masuda, Y., and Sano, H. (1989) Nuclear magnetic resonance and dielectric studies of water adsorbed on synthetic porous alunite. Journal of Physical Chemistry, 93, 7226–7232.

Poplett, I.J.F. and Smith, J.A. (1978) Deuteron quadrupole resonance studies. Journal of the Chemical Society—Faraday Transactions II, 74, 1077–1087.

Ratcliffe, C.I., Ripmeester, J.A., and Tse, J.S. (1985) NMR chemical shifts of dilute ^{1}H in inorganic solids. Chemical Physics Letters, 120, 427–432.

Ripmeester, J.A., Ratcliffe, C.I., Dutrizac, J.E., and Jambor, J.L. (1986) Hydronium ion in the alunite-jarosite group. Canadian Mineralogist, 24, 435–447.

Schukow, H., Breitinger, D.K., Zeiske, T., Kubanek, F., Mohr, J., and Schwab, R.G. (1999) Localization of hydrogen and content of oxonium cations in alunite via neutron diffraction. Zeitschrift für anorganische und allgemeine Chemie, 625, 1047–1050.

Skibsted, J., Nielsen, N.C., Bildsøe, H., and Jakobsen, H.J. (1991) Satellite transitions in MAS NMR spectra of quadrupolar nuclei. Journal of Magnetic Resonance, 95, 88–117.

Smith, M.E. (1993) Application of Al-27 NMR techniques to structure determination in solids. Applied Magnetic Resonance, 4, 1–64.

——— (2000) Recent progress in solid-state NMR of low-gamma nuclei. Annual Reports on NMR Spectroscopy, 43, 121–175.

Soda, G. and Chiba, T. (1969) Deuteron magnetic resonance study of cupric sulfate pentahydrate. Journal of Chemical Physics, 50, 439–455.

Spiess, H.W. (1983) Molecular dynamics of solid polymers as revealed by deuteron NMR. Colloid and Polymer Science, 261, 193–209.

Spiess, H.W. and Sillescu, H. (1981) Solid echoes in the slow-motion region. Journal of Magnetic Resonance, 42, 381–389.

Squyres, S.W., Grotzinger, J.P., Arvidson, R.E., Bell, J.F., Calvin, W., Christensen, P.R., Clark, B.C., Crisp, J.A., Farrand, W.H., Herkenhoff, K.E., Johnson, J.R., Klingelhofer, G., Knoll, A.H., McLennan, S.M., McSween, H.Y., Morris, R.V., Rice, J.W., Rieder, R., and Soderblom, L.A. (2004) In situ evidence for an ancient aqueous environment at Meridiani Planum, Mars. Science, 306(5702), 1709–1714.

Stebbins, J.F., Du, L.-S., Kroeker, S., Neuhoff, P., Rice, D., Frye, J., and Jakobsen, H.J. (2002) New opportunities for high-resolution solid-state NMR spectroscopy of oxide materials at 21.1 and 18.8 T Fields. Solid State Nuclear Magnetic Resonance, 21, 105–115.

Stoffregen, R.E., Alpers, C.N., and Jambor, J.L. (2000) Alunite-jarosite crystallography, thermodynamics, and geochronology. In C.N. Alpers, J.L. Jambor, and D.K. Nordstrom, Eds., Sulfate Minerals—Crystallography, Geochemistry and Environmental Significance, 40, p. 453–479. Reviews in Mineralogy and Geochemistry, Mineralogical Society of America, Chantilly, Virginia.

Wang, R., Bradley, W.F., and Steinfink, H. (1965) The crystal structure of alunite. Acta Crystallographica, 18, 249–252.

Weintraub, O. and Vega, S. (1995) Dynamic ^{2}H nuclear magnetic resonance of rotating solids. Solid State Nuclear Magnetic Resonance, 4, 341–351.

MANUSCRIPT RECEIVED AUGUST 9, 2006
MANUSCRIPT ACCEPTED NOVEMBER 14, 2006
MANUSCRIPT HANDLED BY MICHAEL FECHTELKORD